

## Variable viscosity and thermal conductivity effects on heat transfer by natural convection from a cone and a wedge in porous media

I. A. HASSANIEN<sup>(1)</sup>, A. H. ESSAWY<sup>(2)</sup>, N. M. MOURSY<sup>(2)</sup>

<sup>(1)</sup> Assuit University, Faculty of Science, Department of Mathematics, Assuit, Egypt

<sup>(2)</sup> Minia University, Faculty of Science, Department of Mathematics, Minia, Egypt

THE PROBLEM OF STEADY, laminar heat transfer by natural convection flow over a vertical cone and a wedge embedded in a uniform porous medium with variable viscosity and thermal conductivity is investigated. The transformed governing equations are solved numerically by using a finite difference scheme. The obtained results are compared with earlier papers on special cases of the problem and are found to be in excellent agreement. The influence of porous medium inertia effect, viscosity variation parameter  $\epsilon$  and thermal conductivity variation parameter  $\gamma$  on the fluid velocity and temperature is discussed. Including the porous medium inertia effect or viscosity variation parameter in the mathematical model is predicted to reduce the local Nusselt number. Furthermore, the local Nusselt number increases in the presence of thermal conductivity variation parameter.

### Notations

- $c_p$  specific heat,
- $f$  dimensionless stream function,
- $F$  inertia coefficient of the porous medium,
- $g$  gravitational acceleration,
- $h$  local heat transfer coefficient,
- $K$  permeability of the porous media,
- $\kappa$  thermal conductivity of the porous medium,
- $\kappa_f$  thermal conductivity of the ambient fluid,
- $n$  geometric factor,
- $Nu_x$  local Nusselt number,
- $Ra_x$  local Raleigh number,  $\frac{g \cos \gamma_1 \beta_T K (T_w - T_\infty) x}{\mu_f \alpha_e}$ ,
- $Ra_L$  Raleigh number based on the characteristic length,  $\frac{g \cos \gamma_1 \beta_T K (T_w - T_\infty) L}{\mu_f \alpha_e}$ ,
- $T$  temperature,
- $T_w$  wall temperature,
- $u$  tangential velocity,
- $v$  normal velocity,

|       |   |
|-------|---|
| $V_w$ | wall mass flux coefficient,               |
| $x$   | distance along the cone or the wedge,     |
| $y$   | distance normal to the cone or the wedge. |

### *Greek symbols*

|            |   |
|------------|---|
| $\alpha_e$ | effective thermal diffusivity of the porous medium, $\frac{\kappa_f}{\rho c_p}$ |
| $\beta_T$  | thermal expansion coefficient,  |
| $\epsilon$ | viscosity variation parameter,  |
| $\gamma$   | thermal conductivity variation parameter,                                       |
| $\gamma_1$ | half angle of the cone or the wedge,  |
| $\eta$     | pseudo-similarity variable,   |
| $\Gamma$   | dimensionless porous medium inertia coefficient,                                |
| $\mu$      | dynamic viscosity,  |
| $\mu_f$    | dynamic viscosity of the ambient fluid,   |
| $\theta$   | dimensionless temperature,  |
| $\rho$     | density,  |
| $\xi$      | dimensionless distance,   |
| $\psi$     | stream function.  |

### *Subscripts*

|          |                        |
|----------|------------------------|
| $w$      | condition at the wall, |
| $\infty$ | condition at infinity. |

## 1. Introduction

FLOW AND HEAT transfer from different geometries embedded in porous media have many engineering and geophysical applications such as geothermal reservoirs, drying of porous solids, thermal insulation, enhanced oil recovery, packed-bed catalytic reactors, cooling of nuclear reactors, and underground energy transport. Most early studies on porous media have used the Darcy law, which is a linear empirical relationship between the Darcian velocity and the pressure drop across the porous medium and is limited to slow flows. However, for high velocity flow situations, the Darcy law is inapplicable because it does not account for the resulting inertia effects of the porous medium. In this situation, the relationship between the velocity and the pressure drop is quadratic. The high flow situation is established when the Reynolds number based on the pore size is greater than unity. VAFAI and TIEN [1] have discussed the importance of inertia effects for flows in porous media.

CHENG and MINKOWYCZ [2] have used the Darcy law in their study on free convection about a vertical impermeable flat plate in porous medium. CHENG *et al.* [3] have analyzed the problem of natural convection of a Darcian flow about a cone using the local nonsimilarity method. CHAMKHA [4] has obtained similarity solutions for the problem of non-Darcy free convection from a nonisothermal

cone and a wedge in a porous medium. YIH [5] has reported the effect of uniform lateral mass flux on free convection about a vertical cone embedded in a fluid-saturated porous medium. HOSSAIN *et al.* [6] have studied non-Darcy natural convection heat and mass transfer along a vertical permeable cylinder embedded in a porous medium. YIH [7] studied coupled heat and mass transfer in mixed convection about a wedge embedded in saturated porous medium. CHAMKHA [8] has studied simultaneous heat and mass transfer by natural convection about a vertical wedge and a cone embedded in a porous medium.

In all of the papers mentioned above the viscosity and thermal conductivity are assumed as constant. However, the problem of mixed convection flow past a wedge for temperature-dependent viscosity was investigated by HOSSAIN *et al.* [9]. HASSANIEN [10] analyzed the problem of mixed convection from impermeable vertical wedge in a fluid-saturated porous medium incorporating the variation of permeability and thermal conductivity. HOSSAIN and MUNIR [11] have investigated the natural convection flow of a viscous incompressible fluid from an isothermal truncated cone. HOSSAIN *et al.* [12] have studied the effect of radiation on free convection flow of fluid with variable viscosity from a porous vertical plate.

The aim of the present work is to study the variable viscosity and thermal conductivity effects on heat transfer by natural convection about an isothermal vertical wedge and cone embedded in a fluid-saturated porous medium. A nonsimilarity transformation is employed to transform the governing differential equations to a form whereby they produce their own initial conditions. The transformed equations are solved numerically. The obtained results for special cases of the problem were compared with the previously published work and were found to be in excellent agreement.

## 2. Problem definition

Consider steady, laminar, heat transfer by natural convection flow over a stationary permeable cone embedded in a fluid-saturated porous medium. Figure 1 shows the schematic diagram of the problem. The origin of the coordinate system is placed at the vertex of the cone, where the  $x$ -direction is taken along the cone and the  $y$ -direction is normal to the cone. The fluid is assumed to be Newtonian and has constant properties except the density in the buoyancy term of the balance of momentum equation, the viscosity and thermal conductivity. The fluid and the porous medium are assumed to be in local thermal equilibrium. The surface of the cone is kept at constant wall temperature. The temperature at the cone surface is always greater than its uniform ambient values existing far from the cone surface.

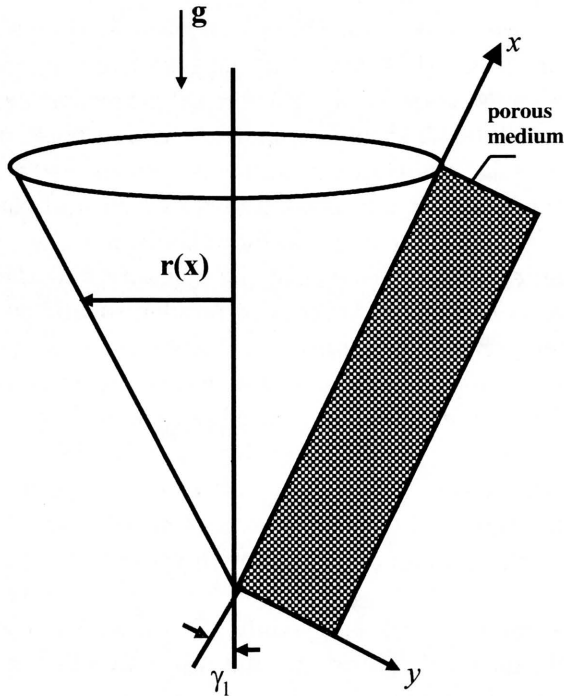


FIG. 1. Flow model and physical coordinate system.

The governing equations that take into account the inertia effects of the porous medium within the boundary layer and Boussinseq approximations may be written as follows:

$$(2.1) \quad \frac{\partial r^n u}{\partial x} + \frac{\partial r^n v}{\partial y} = 0,$$

$$(2.2) \quad \left[ 1 + 2 \frac{FK}{\mu} u \right] \frac{\partial u}{\partial y} = \mu u \frac{d}{dy} \left( \frac{1}{\mu} \right) + \frac{\rho g \beta_T K \cos \gamma_1}{\mu} \frac{\partial T}{\partial y},$$

$$(2.3) \quad u \frac{\partial T}{\partial x} + v \frac{\partial T}{\partial y} = \frac{1}{\rho c_p} \frac{\partial}{\partial y} \left( \kappa \frac{\partial T}{\partial y} \right),$$

The boundary conditions are defined as follows:

$$(2.4) \quad v = V_w, \quad T = T_w \quad \text{at} \quad y = 0,$$

$$(2.5) \quad u = 0, \quad T = T_\infty \quad \text{at} \quad y \rightarrow \infty,$$

where  $u$  and  $v$  are velocities in the  $x$  and  $y$  directions,  $\rho$  is the density,  $c_p$  is the specific heat,  $g$  is the gravitational acceleration,  $K$  is the permeability of the porous medium,  $\beta_T$  is the thermal expansion coefficient of the fluid,  $T$  is the temperature,  $F$  is the inertia coefficient of the porous medium, the value  $V_w$  (constant) is the surface mass flux coefficient. The value of  $n$  can be either  $n = 0$  for a flow over a vertical wedge or  $n = 1$  for a flow over a vertical cone. When  $n = 0$  and  $\gamma = 0$ , the problem will reduce to the case of a vertical flat plate. The above equations were derived under the assumption that the boundary-layer thickness is sufficiently thin compared to the local radius of the cone. Thus, the local radius at a point in the boundary layer can be replaced by the radius of the cone ( $x = r \sin \gamma_1$ ).

Following [11], the variation of dynamic viscosity and thermal conductivity with the temperature are written in the form:

$$(2.6) \quad \mu = \mu_f \left[ 1 + \frac{1}{\mu_f} \left( \frac{d\mu}{dT} \right)_f (T - T_\infty) \right],$$

$$(2.7) \quad \kappa = \kappa_f \left[ 1 + \frac{1}{\kappa_f} \left( \frac{d\kappa}{dT} \right)_f (T - T_\infty) \right],$$

where the subscript  $f$  denotes the quantities outside the boundary layers. Introducing the following dimensionless variables:

$$(2.8) \quad \xi = \frac{2V_w}{\alpha_e \sqrt{\text{Ra}_x}},$$

$$(2.9) \quad \eta = \frac{y}{x} \sqrt{\text{Ra}_x},$$

$$(2.10) \quad f(\xi, \eta) = \frac{\psi}{\alpha_e r^n \sqrt{\text{Ra}_x}},$$

$$(2.11) \quad \theta(\xi, \eta) = \frac{T - T_\infty}{T_w - T_\infty},$$

and substituting Eqs. (2.8)–(2.11) into Eqs. (2.1)–(2.3) we obtain the following transformed governing equations:

$$(2.12) \quad \left[ 1 + \frac{\Gamma}{1 + \epsilon \theta} f' \right] f'' = \frac{1}{1 + \epsilon \theta} [-\epsilon f' \theta' + \theta'],$$

$$(2.13) \quad [1 + \gamma \theta] \theta'' + \left( n + \frac{1}{2} \right) f \theta' + \gamma \theta'^2 = \frac{\xi}{2} \left( f' \frac{\partial \theta}{\partial \xi} - \theta' \frac{\partial f}{\partial \xi} \right),$$

with the boundary conditions transformed to:

$$(2.14) \quad f = \frac{\xi}{2n+2}, \quad \theta = 1 \quad \text{at} \quad \eta = 0,$$

$$(2.15) \quad f' = 0, \quad \theta = 0 \quad \text{at} \quad \eta \rightarrow \infty,$$

where the primes denote partial derivatives with respect to  $\eta$ ,  $\Gamma = \frac{2FK\alpha_e Ra_L}{\mu_f L}$  is dimensionless porous medium inertia coefficient,  $\epsilon = \frac{1}{\mu_f} \left( \frac{d\mu}{dT} \right)_f (T_w - T_\infty)$  is the viscosity variation parameter,  $\gamma = \frac{1}{\kappa_f} \left( \frac{d\kappa}{dT} \right)_f (T_w - T_\infty)$  is the thermal conductivity variation parameter, and  $\alpha_e$  is the equivalent thermal diffusivity. The kind of the applicable fluid for the present form of viscosity and thermal conductivity is discussed in more detail is given in [11, 14]. The velocity components are given by:

$$(2.16) \quad u = \frac{\alpha_e Ra_x}{x} f',$$

$$(2.17) \quad v = -\frac{\alpha_e \sqrt{Ra_x}}{x} \left[ (2n+1)f + \xi \frac{\partial f}{\partial \xi} + \eta f' \right].$$

The local Nusselt number  $Nu_x$  is given by:

$$(2.18) \quad \frac{Nu_x}{\sqrt{Ra_x}} = -(1+\gamma)\theta'(\xi, 0).$$

We now obtain approximate solutions of the equations (2.12)–(2.13) based on the local similarity and non-similarity methods [13]. For the first level of truncation the  $\xi$  derivatives in equation (2.13) can be neglected. Thus, the governing equations for the first level of the truncation are equation (2.12) and the following equation:

$$(2.19) \quad [1 + \gamma\theta] \theta'' + \left( n + \frac{1}{2} \right) f \theta' + \gamma \theta'^2 = 0$$

subject to the boundary conditions

$$(2.20) \quad f = -\frac{\xi}{2n+2}, \quad \theta = 1 \quad \text{at} \quad \eta = 0,$$

$$(2.21) \quad f' = 0, \quad \theta = 0 \quad \text{at} \quad \eta \rightarrow \infty.$$

At the second level of truncation, we introduce  $\Pi = \frac{\partial f}{\partial \xi}$ ,  $\Phi = \frac{\partial \theta}{\partial \xi}$  and restore all of neglected terms in the first level of truncation; thus, we have Eq. (2.12) and the following equation:

$$(2.22) \quad [1 + \gamma\theta]\theta'' + \left(n + \frac{1}{2}\right) f\theta' + \gamma\theta'^2 = \frac{\xi}{2} (f'\Phi - \theta'\Pi)$$

subject to the boundary conditions

$$(2.23) \quad f = \frac{\xi}{2n+2}, \quad \theta = 1 \quad \text{at} \quad \eta = 0,$$

$$(2.24) \quad f' = 0, \quad \theta = 0 \quad \text{at} \quad \eta \rightarrow \infty.$$

The introduction of the two new dependent variables  $\Pi$  and  $\Phi$  in the problem requires two equations with appropriate boundary conditions. This can be obtained by differentiating (2.12) and (2.13) with respect to  $\xi$  and neglecting the terms  $\frac{\partial^2 f}{\partial \xi^2}$  and  $\frac{\partial^2 \theta}{\partial \xi^2}$  which leads to

$$(2.25) \quad \left[1 + \frac{\Gamma}{1 + \epsilon\theta}\right] \Pi'' - \frac{\epsilon\Gamma}{(1 + \epsilon\theta)^2} \Phi f'' \\ = \frac{1}{1 + \epsilon\theta} [-\epsilon(f'\Phi' + \Pi'\theta') + \Phi'] - \frac{\epsilon\Phi}{(1 + \epsilon\theta)^2} [-\epsilon f'\theta' + \theta'],$$

$$(2.26) \quad (1 + \gamma\theta)\Phi'' + \gamma\Phi\theta'' + \left(n + \frac{1}{2}\right) (\Pi\theta' + f\Phi') + 2\gamma\theta'\Phi' \\ = \frac{\xi}{2} (\Pi\Phi - \Phi'\Pi) + \frac{1}{2} (f'\Phi - \theta'\Pi),$$

with boundary conditions

$$(2.27) \quad \Pi = \frac{1}{2n+2}, \quad \Phi = 0 \quad \text{at} \quad \eta = 0,$$

$$(2.28) \quad \Pi' = 0, \quad \Phi = 0 \quad \text{at} \quad \eta \rightarrow \infty.$$

The resulting equations with the boundary conditions have been solved numerically using a finite difference method.

3. Results and discussion

Numerical results are obtained for  $\epsilon = 0,5$ ,  $\gamma = 0,2.5$ ,  $\Gamma = 0,0.5$ , and  $n = 0,1$ . In order to verify the accuracy of our present method, we have compared our results with those of YIH [5] and CHAMKHA *et al.* [7]. The present results compared with the above researches are in good agreement, as shown in Table 1. Table 2 gives the parametric conditions for each of the curves shown in Figs. 2–5.

**Table 1.** Values for  $-\theta'(\xi, 0)$  for the cases of wedge  $n = 0$  and cone  $n = 1$  with  $(\Gamma = 0, \epsilon = 0, \gamma = 0)$ .

| $\xi$ | $n = 0$ |                           |                 | $n = 1$ |                           |                 |
|-------|---------|---------------------------|-----------------|---------|---------------------------|-----------------|
|       | YIH [5] | CHAMKHA <i>et al.</i> [7] | Present results | YIH [5] | CHAMKHA <i>et al.</i> [7] | Present results |
| -10   | 4.9999  | 4.9830                    | 5.0008          | 5.0995  | 5.0857                    | 5.1006          |
| -8    | 3.9999  | 3.9892                    | 4.0015          | 4.1244  | 4.1156                    | 4.1256          |
| -6    | 2.9999  | 2.9936                    | 3.0036          | 3.1655  | 3.1603                    | 3.1661          |
| -4    | 2.0015  | 1.9976                    | 2.0127          | 2.2434  | 2.2409                    | 2.2453          |
| -2    | 1.0725  | 1.0722                    | 1.0810          | 1.4139  | 1.4132                    | 1.4153          |
| 0     | 0.4437  | 0.4439                    | 0.4445          | 0.7686  | 0.7686                    | 0.7687          |
| 2     | 0.1416  | 0.1423                    | 0.1355          | 0.3537  | 0.3541                    | 0.3530          |
| 4     | 0.0333  | 0.0340                    | 0.0229          | 0.1342  | 0.1349                    | 0.1309          |
| 6     | 0.0055  | 0.0058                    | 0.0011          | 0.0400  | 0.0411                    | 0.03559         |
| 8     | 0.0006  | 0.0007                    | 0.000009        | 0.0092  | 0.0096                    | 0.0064          |
| 10    | 0.0001  | 0.0001                    | 0.0             | 0.0016  | 0.0017                    | 0.0006          |

**Table 2.** Parametric values for curves in the figures.

| Curve | $\Gamma$ | $\epsilon$ | $\gamma$ |
|-------|----------|------------|----------|
| I     | 0        | 0          | 0        |
| II    | 0.5      | 0          | 0        |
| III   | 0        | 0          | 2.5      |
| IV    | 0.5      | 0          | 2.5      |
| V     | 0        | 5          | 2.5      |
| VI    | 0.5      | 5          | 2.5      |

Figures 2 and 3 represent the behavior of the stream function and the fluid velocity for the situations shown in Table 2 for both a cone and a wedge at positive lateral wall mass flux at  $\xi = 10$ . A resistance against the flow exists if the porous medium inertia effect is considered. As a result, the flow stream function and velocities near the wall decrease as shown by curves II and IV compared with curves I and III for a cone and a wedge. Also, the effect of viscosity and



thermal conductivity variation parameters on both the stream function and the velocity is observed. It is found that the flow stream functions and velocities near the wall decrease as the viscosity variation parameter  $\epsilon$  or thermal conductivity variation parameter  $\gamma$  increase.

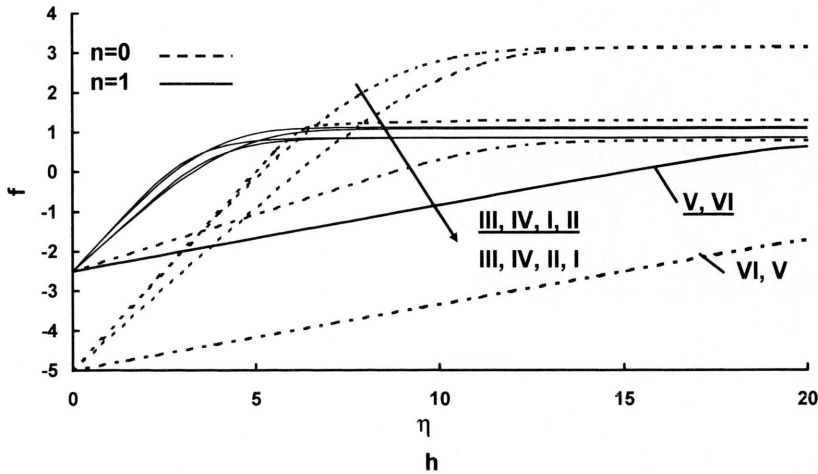


FIG. 2. Stream function distribution for various values of  $\epsilon$ ,  $\gamma$  and  $n$ .

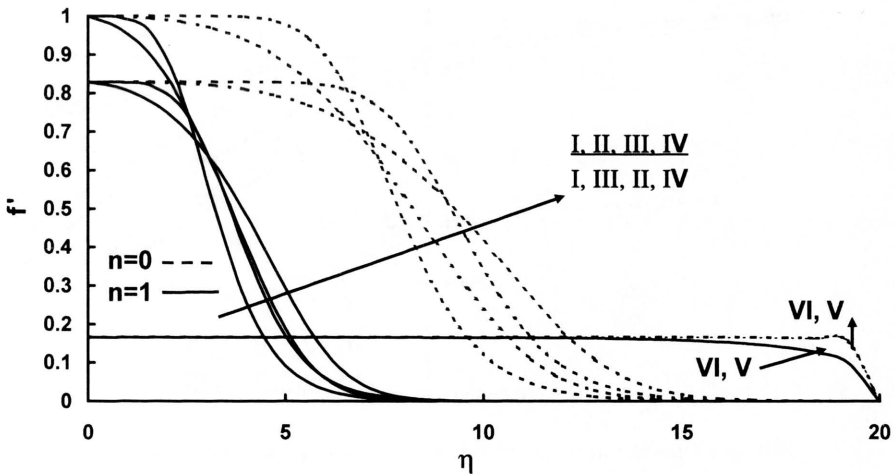


FIG. 3. Velocity distribution for various values of  $\epsilon$ ,  $\gamma$  and  $n$ .

Figure 4 illustrates the temperature profiles for a cone and a wedge at  $\xi = 10$ . The resistive force discussed in the previous paragraph due to the presence of inertia effect tends to increase the temperature of the flow for a wedge and a cone.

It is also seen that the temperature increases as viscosity variation parameter. Also, as thermal conductivity variation parameter increases, the temperature profiles decrease near the wall.

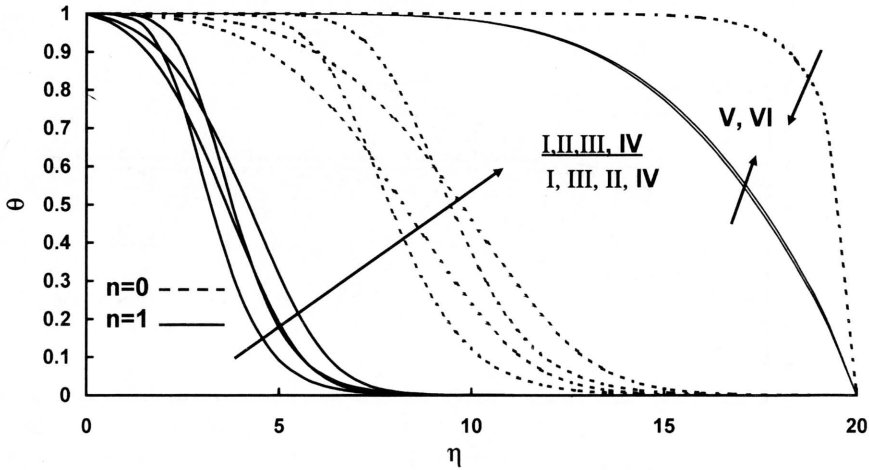


FIG. 4. Temperature distribution for various values of  $\epsilon, \gamma$  and  $n$ .

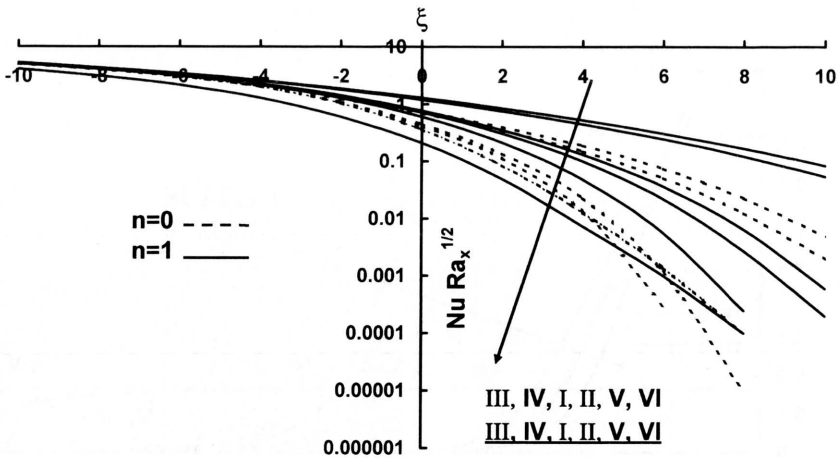


FIG. 5. Nusselt number distribution for various values of  $\epsilon, \gamma$  and  $n$ .

Figure 5 illustrates the distribution of the local Nusselt number for a wedge and a cone. The porous medium inertia effect tends to decrease the local Nusselt number due to its effect on the wall temperature slopes. As viscosity variation parameter increases, the Nusselt number decreases. On the contrary, the Nusselt number increases as thermal conductivity variation parameter  $\gamma$  increases.

#### 4. Conclusions

The problem of steady, laminar heat transfer by natural convection boundary layer flow of variable viscosity and thermal conductivity over an isothermal vertical permeable cone or wedge with constant lateral wall mass flux embedded in a uniform porous medium was considered. The governing equations for uniform wall temperature were developed and transformed by using appropriate nonsimilarity transformations. The transformed equations were solved numerically by using the Keller-Box method. The numerical results are presented. It is found that the Nusselt number decreased when the porous medium inertia or thermal conductivity variation parameter effects are considered. Furthermore, the local Nusselt number increases in the presence of the viscosity variation parameter.

#### References

1. K. VAFAI, C. L. TIEN, *Boundary and inertia effects on flow and heat transfer in porous media*, Int. J. Heat Mass Transfer, **24**, 195–203, 1981.
2. P. CHENG, W. J. MINKOWYCZ, *Free convection about a vertical flat plate embedded in a porous medium with application to heat transfer from a dike*, J. Geophys. **82**, 2040–2044, 1977.
3. P. CHENG, T. LE, I. POP, *Natural convection of a Darcian fluid about a cone*, Int. Commun. Heat Mass Transfer, **12**, 705–717, 1985.
4. A. J. CHAMKHA, *Non-Darcy hydromagnetic free convection from a cone and a wedge in porous media*, Int. Comm. Heat Mass Transfer, **23**, 875–887, 1996.
5. K. A. YIH, *The effect of uniform lateral mass flux on free convection about a vertical cone embedded in a porous media*, Int. Commun. Heat Mass Transfer, **24**, 1195–1205, 1997.
6. M. A. HOSSAIN, K. VAFAI, K. KHANAFER, *Non-Darcy natural convection heat and mass transfer along a vertical permeable cylinder embedded in a porous medium*, Int. J. Thermal Sci., **38**, 854–862, 1999.
7. K. A. YIH, *Coupled heat and mass transfer in mixed convection over a VHF/VMF wedge in porous media: the entire regime*, Acta Mechanica, **137**, 1–12, 1999.
8. A. J. CHAMKHA, A. R. A. KHALED, O. AL-HAWAJ, *Simultaneous heat and mass transfer by natural convection from a cone and a wedge in porous media*, J. Porous Media, **3**, 155–164, 2000.
9. M. A. HOSSAIN, M. S. MUNIR, D. A. S. REES, *Flow of viscous incompressible fluid with temperature-dependent viscosity and thermal conductivity past a permeable wedge with uniform surface heat flux*, Int. J. Thermal Sci., **39**, 635–644, 2000.
10. I. A. HASSANIEN, *Variable permeability effects on mixed convection along a vertical wedge embedded in a porous medium with variable surface heat flux*, Applied Mathematics and Computation, **138**, 41–59, 2003.
11. M. A. HOSSAIN, M. S. MUNIR, *Natural convection flow of a viscous fluid about a truncated cone with temperature-dependent viscosity and thermal conductivity*, Int. J. Num. Methods. Heat Fluid Flow, **11**, 494–510, 2001.

12. M. A. HOSSAIN, K. KHANAFER, K. VAFAI, *The effect of radiation on free convection flow of fluid with variable viscosity from a porous vertical plate*, Int. J. Thermal Sci. **40**, 115–124, 2001.
13. E. M. SPARROW, H. QUACK, J. BOERNER, *Local non-similarity boundary solutions*, AIAA, **8**, 1936–1942, 1970.
14. P. L. GELRINGER, *Hand book of heat transfer medium*, New York 1962.

Received February 28, 2002; revised version June 6, 2003.

---